Supporting information:

Tuneable and efficient manufacturing of Li-ion battery separators using photopolymerization-induced phase separation

Samuel Emilsson,[a] Göran Lindbergh [b] and Mats Johansson [a]*

[a.] *Division of Coating Technology, Department of Fibre and Polymer Technology, KTH Royal Institute of Technology, SE-100 44 Stockholm, Sweden*
[b.] *Division of Applied Electrochemistry, Department of Chemical Engineering, KTH Royal Institute of Technology, SE-100 44 Stockholm, Sweden*

Table S1: Chemical compositions (w/w) of all the thermoset membranes that were screened

Sample	TEG	PC	BMA	TEMPIC
TEGPC-1-30%	0.15	0.15	0.7	0
TEGPC-1-40%	0.2	0.2	0.6	0
TEGPC-1-50%	0.25	0.25	0.5	0
TEGPC-1-60%	0.3	0.3	0.4	0
TEGPC-2-30%	0.2	0.1	0.7	0
TEGPC-2-40%	0.27	0.13	0.6	0
TEGPC-2-50%*	0.33	0.17	0.5	0
TEGPC-2-60%	0.4	0.2	0.4	0
TEGPC-4-30%	0.24	0.06	0.7	0
TEGPC-4-40%	0.32	0.08	0.6	0
TEGPC-4-50%	0.4	0.1	0.5	0
TEGPC-4-60%	0.48	0.12	0.4	0
TEGPC-4-40%-5T	0.4	0.1	0.57	0.03
TEGPC-4-40%-10T	0.4	0.1	0.54	0.06
TEGPC-4-40%-20T	0.4	0.1	0.48	0.12
TEGPC-2-50%-10T	0.33	0.17	0.45	0.05

*This formulation was also investigated on glass substrates without a PVA coating – see Figure S2

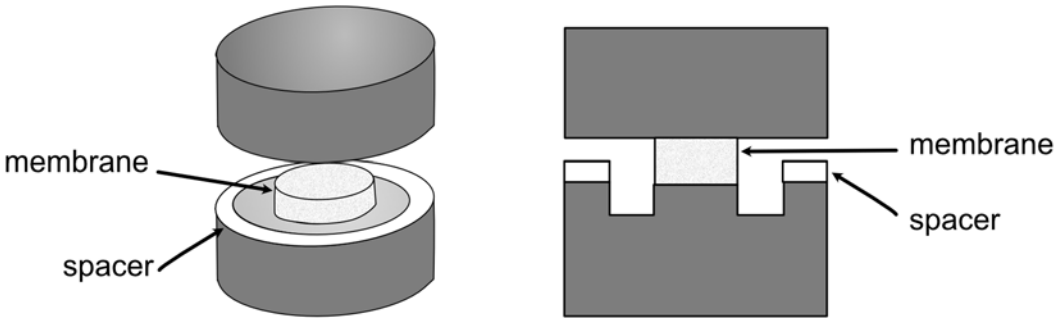

Figure S1: EIS setup for measuring effective conductivity through membranes. The figure shows the inner parts of the Swagelok cell.

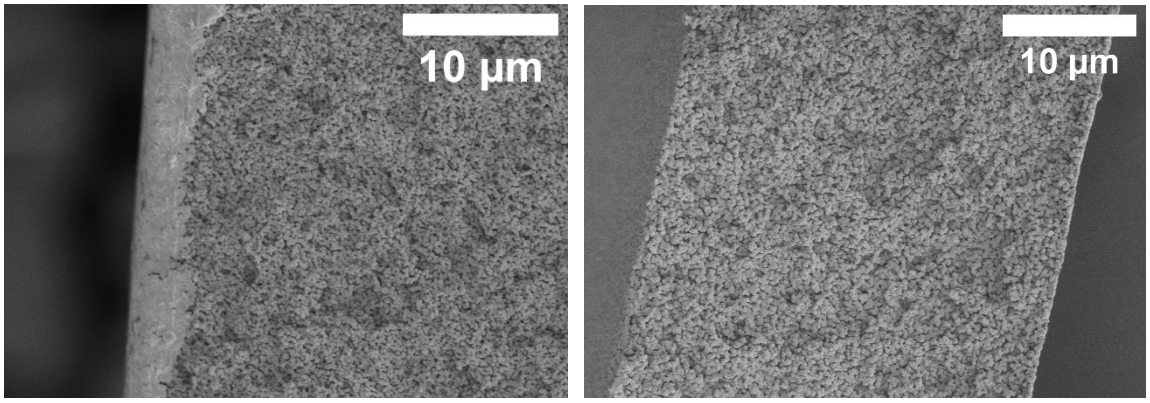

Figure S2: Left: SEM micrograph of cross-section of TEGPC-2-50% membrane containing a non-porous surface film manufactured using glass without a PVA coating. (3.5k magnification). Right: SEM micrograph of cross-section of full TEGPC-2-50% membrane manufactured using PVA coated glass, without any non-porous surface film (3k magnification)

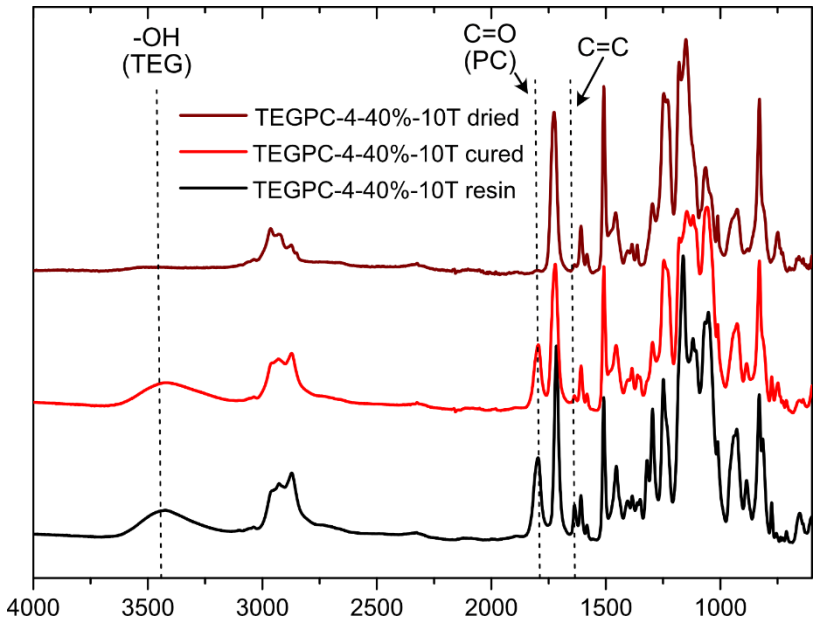

Figure S3: Full FTIR spectra of the formulation TEGPC-4-40% in the uncured resin state, the wet cured film and the cured dried film.

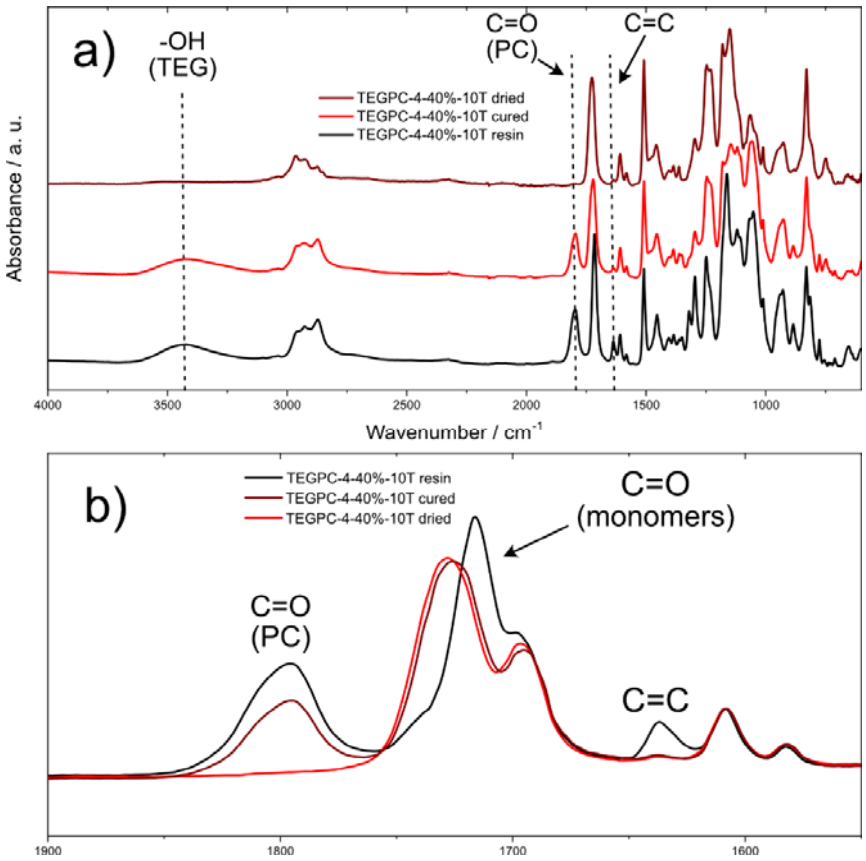

Figure S4: a) Full FTIR spectra of the formulation TEGPC-4-40%-10T in the uncured resin state, the wet cured film and the cured dried film and b) shows a selected region to follow the disappearance of the double bond stretch at 1637 cm^{-1}.

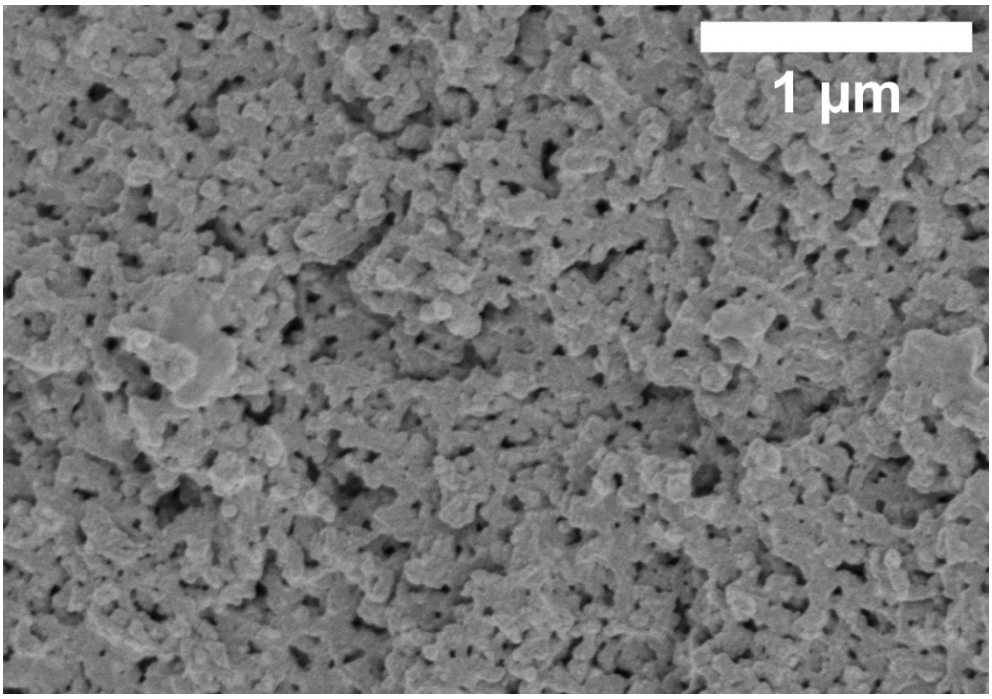

Figure S5: SEM micrograph of the cross-section of TEGPC-4-30% at 35,000 x magnification. This shows that a porous structure is obtain even at low porogen content (30wt%) when using a larger content of TEG.

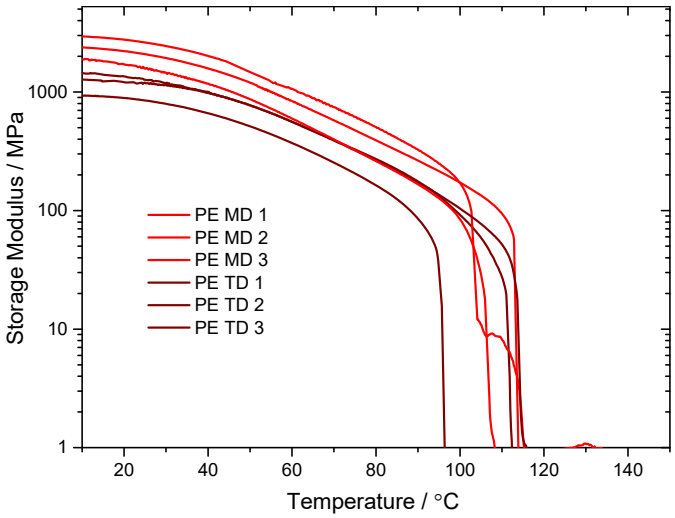

Figure S6: DMA thermograph of different runs of the PE references material showing a large spread in storage modulus and drop off temperature due to the low thickness (20 µm) of the material.

Table S2: Conductivity of TEGPC4-40% using different liquid electrolytes

Sample		Ionic conductivity / mS cm^{-1} (25 °C)	N_M
TEGPC41-40% w/ EC/DEC 1M $LiPF_6$	Film	0.99	4.9
	LE	4.9	
TEGPC41-40% w/ EC/PC 1M LiTFSI	Film	0.87	4.9
	LE	4.3	

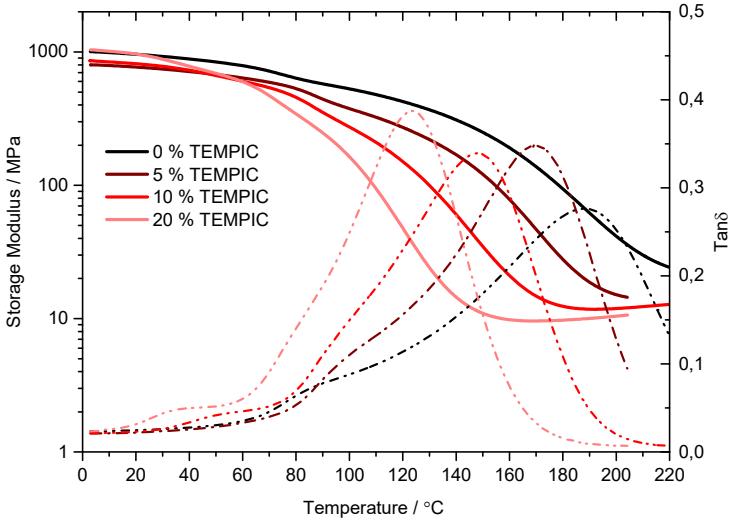

Figure S7: DMA thermograph of formulations of TEGPC4-40% with increasing contain of TEMPIC monomer. The tanδ peak indicates the T_g of the formulation.

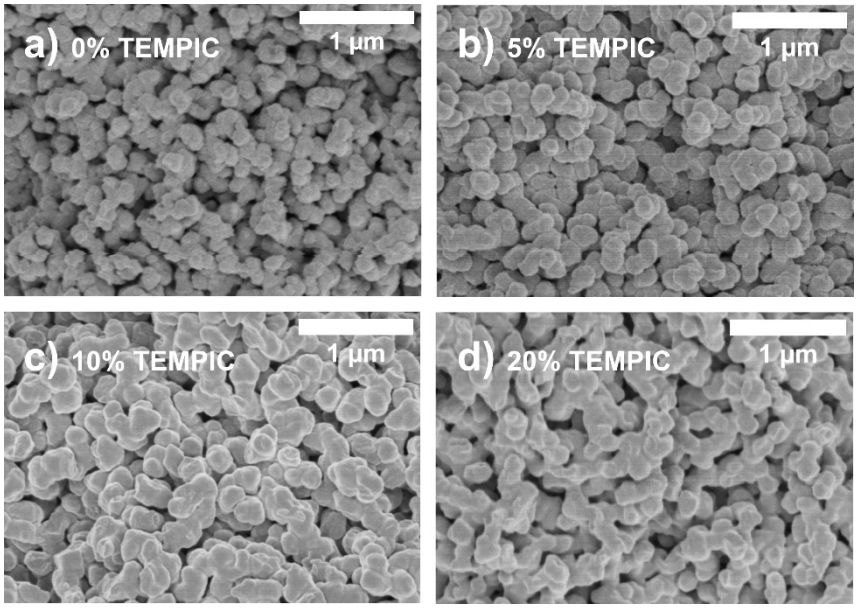

Figure S8: SEM micrographs of the cross-section of a) TEGPC-4-40% b) TEGPC-4-40%-5T c) TEGPC-4-40%-10T d) TEGPC-4-40%-20T at 35,000 x magnification

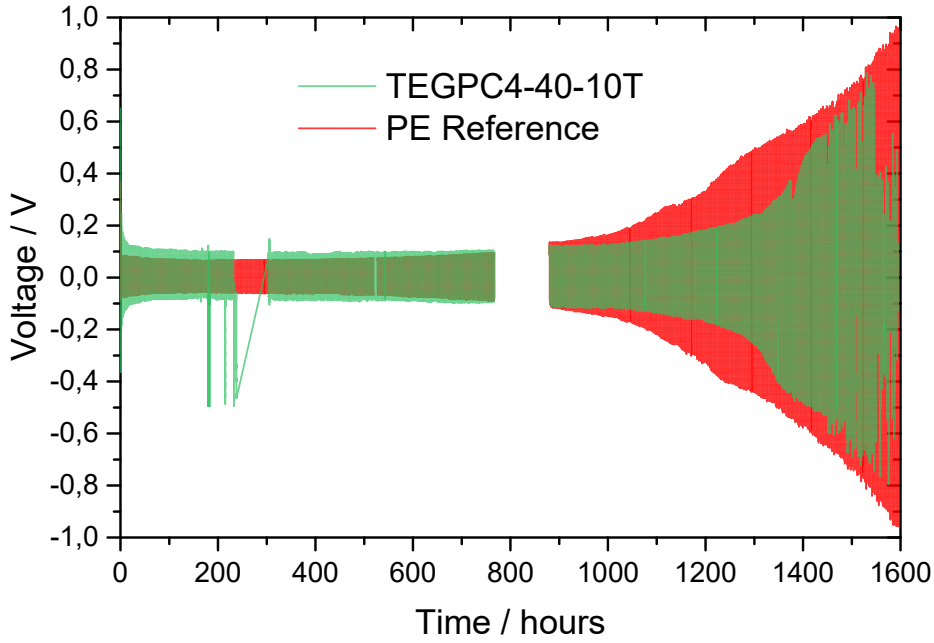

Figure S9: Voltage profiles of Li-Li symmetrical cell cycling at 0.5 mA cm^{-1} (0.5 mAh cm^{-1}) with PE reference and TEGPC-4-40%-10T for 1600 hours. Due to issues with the potentiostat, the data for hours 232-308 for TEGPC-4-40%-10T and hours 768-882 for TEGPC-4-40%-10T and PE reference was lost. Data from the applied current shows that it continued to cycle and age.

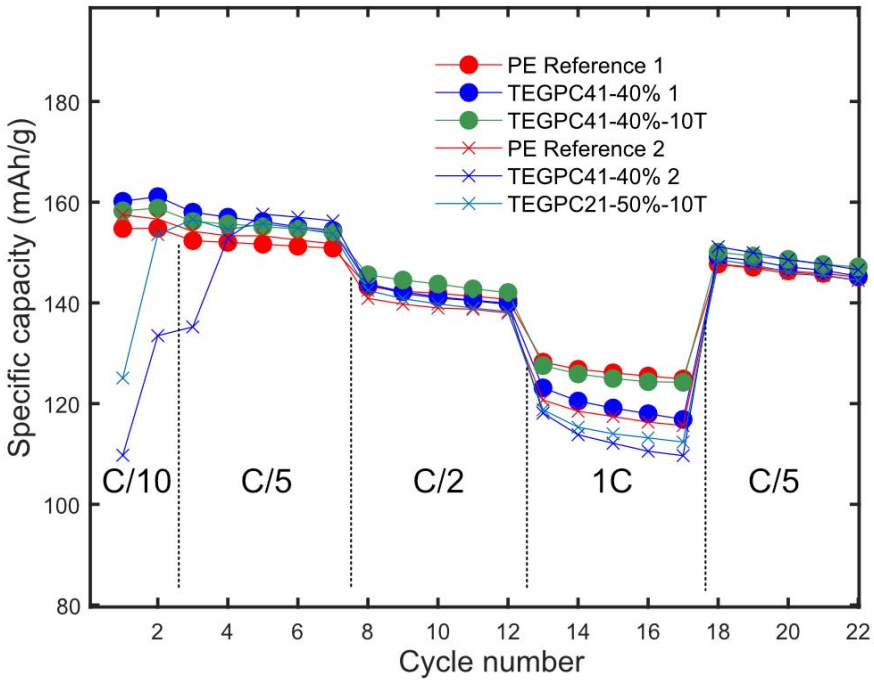

Figure S10: Capacity retention test for several different formulations of thermoset membranes and the PE reference. Cells were cycled between 2.6 and 3.9 V and two formation cycles at C/10 were used. Note that the batch to batch difference for the PE reference is rather large, related to varying glovebox conditions during study.